European Journal of Mechanics / B Fluids 77 (2019) 171–176

Contents lists available at ScienceDirect

European Journal of Mechanics / B Fluids

journal homepage: www.elsevier.com/locate/ejmflu

Non-modal Floquet stability of capsules in large-amplitude oscillatory extensional flow

Spencer H. Bryngelson [a,*], Jonathan B. Freund [a,b]

[a] Department of Mechanical Science & Engineering, University of Illinois at Urbana–Champaign, Urbana, IL 61801, USA
[b] Department of Aerospace Engineering, University of Illinois at Urbana–Champaign, Urbana, IL 61801, USA

ARTICLE INFO

Article history:
Received 5 November 2018
Received in revised form 14 March 2019
Accepted 20 April 2019
Available online xxxx

ABSTRACT

We analyze the stability of a capsule in large-amplitude oscillatory extensional (LAOE) flow, as often used to study the rheology and dynamics of suspensions. Such a flow is typically established in a cross-slot configuration, with the particle (or particles) of interest observed in the stagnation region. However, controlling this configuration is challenging because the flow is unstable. We quantify such an instability for spherical elastic capsules suspended near the stagnation point using a non-modal global Floquet analysis, which is formulated to include full coupling of the capsule-viscous-flow dynamics. The flow is shown to be transiently, though not asymptotically, unstable. For each case considered, two predominant modes of transient amplification are identified: a predictable intra-period growth for translational capsule perturbations and period-to-period growth for certain capsule distortions. The amplitude of the intra-period growth depends linearly on the flow strength and oscillation period, which corresponds to a shift of the flow stagnation point, and the period-to-period growth saturates over several periods, commensurate with the asymptotic stability of the flow.

1. Introduction

Oscillatory rheometry is often used to measure the properties of polymer solutions and blends [1,2], melts [3], and colloidal [4] and capsule suspensions [5,6]. We consider the specific case of the large-amplitude oscillatory extensional (LAOE) flow shown in Fig. 1, which has been used to quantify nonlinear viscoelastic and extensional phenomena, such as the unraveling and alignment of flexible bio-filaments [7]. LAOE flow experiments are straightforward in bulk-fluids, such as melts and cross-linked polymer networks [8,9], but single-particle studies are more challenging. A sophisticated control mechanism seems to be necessary to stabilize the particle position for observation [10–13]. Though complex, such techniques have enabled analysis of polymer strands such as DNA [14,15]. Quantifying the instabilities of this flow, especially when the particles of interest are themselves complex, is challenging though potentially informative for the design of such microfluidic traps. Here, we investigate this instability directly through a linear Floquet analysis of a model flow system.

We take elastic capsules – liquid filled thin membranes – as canonical suspended soft particles (visualized in Fig. 1). Natural capsules include cells, vesicles, and viruses, though microcapsules can also be manufactured. Recent efforts have developed capsules for cosmetic creams [16,17], release of aromas and flavors [18–20], absorption of CO_2 in gas plumes [21], targeted drug delivery [22–25], contrast-enhanced ultrasound [26], and artificial blood and organ development [27–29]; this broad set of applications motivates our study.

The stability of capsules in similar, though steady, flows has been assessed through numerical simulation [30–33] and experiment [34,35]. Shape instabilities of elongated axisymmetric capsules in uniaxial extension have been identified, with their conformation and associated growth rates depending upon the flow strength and at-rest capsule shape; sufficiently round shapes are stable for all flow strengths considered [30]. However, capsules in oscillatory flow can exhibit qualitatively different behaviors than the steady-flow version of the same system. Such differences can affect the stability; for example, ellipsoidal and biconcave capsules in oscillatory shear flow [36–38] have markedly different stability behaviors when compared to steady shear flow [39–42]. We thus anticipate differences in the stability of capsules in steady and oscillatory extensional flow.

The model capsule flow system is introduced in Section 2.1. A spectral boundary integral method, which includes full coupling between the elastic capsule membrane and surrounding fluid, is used to discretize and solve for the flow as described in Section 2.2. In Section 2.3 we present the time-periodic base-flows to be analyzed. A linear, global, non-modal Floquet analysis is formulated in Section 3. We verify our formulation and implementation against direct numerical simulations (DNS) and assess

* Corresponding author.
E-mail addresses: spencer@caltech.edu, sbryngelson@gmail.com (S.H. Bryngelson).

https://doi.org/10.1016/j.euromechflu.2019.04.012
0997-7546/

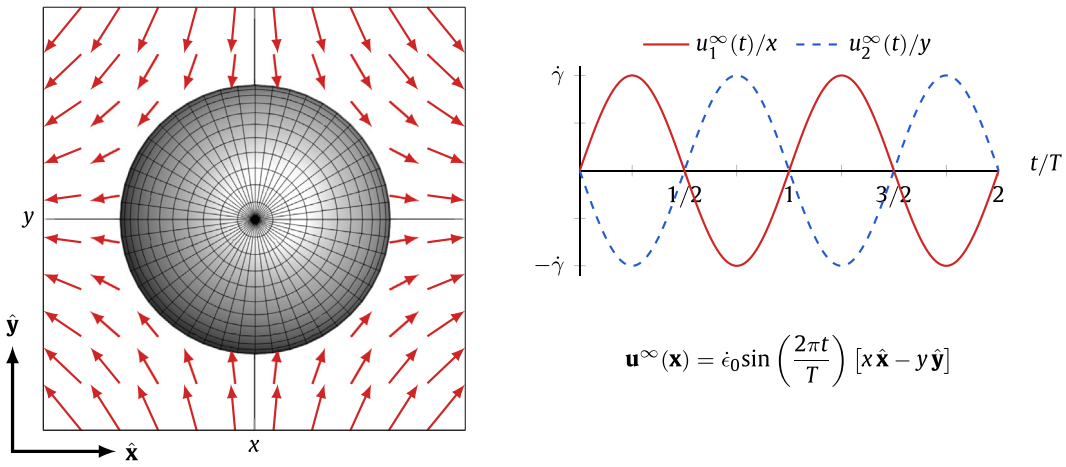

Fig. 1. Schematic of the model system and velocity field $\mathbf{u}^\infty(\mathbf{x})$.

the capsule stability for different flow strengths and frequencies in Section 4.

2. Model system and flow solution

2.1. Simulation setup

We consider an (at-rest) spherical elastic capsule of radius r_o subject to oscillatory planar extensional flow, as shown in Fig. 1. The velocity field is visualized in Fig. 1 and has maximum strain rate $\dot{\epsilon}_0$ and period T. The interior and exterior fluids are incompressible and Newtonian with matching viscosity μ.

The capsule membrane elasticity is described using a Skalak constitutive model [43] with linear shear and dilatation moduli, E_s and $E_d = 10E_s$, respectively. Bending is resisted by a linear isotropic model with respect to a spherical reference shape and modulus $E_b = 5 \times 10^{-3} E_s r_o^2$ [44], which is representative of actual capsule membranes [45]. Together, these parameters give a characteristic capsule relaxation time $\tau = \mu r_o / E_s$. A corresponding Weissenberg number is $Wi = \tau \dot{\epsilon}_0$, and serves as a measure of relative flow strength, and a Deborah number is $De = \tau/T$, which is a ratio of capsule to flow time scales.

2.2. Flow solution

The capsule geometry $\mathbf{x}$ is represented by spherical harmonics as

$$\mathbf{x}(\theta,\phi) = \sum_{n=0}^{N-1} \sum_{m=0}^{n} \widetilde{P}_n^m(\sin\theta)(\mathbf{a}_{nm}\cos m\phi + \mathbf{b}_{nm}\sin m\phi), \tag{1}$$

where $\widetilde{P}_n^m$ are the normalized Legendre polynomials. This description is advantageous in that few modes are required to accurately describe the capsule shape and it enables a nondissipative dealiasing procedure for nonlinear numerical stability of the flow simulations [44]. Most importantly for the present analysis, the orthogonality of the spherical harmonic modes facilitates our stability analysis as discussed in Section 3. The total number of modes is $3N^2$, where $N = 6$ is used for all reported results, though we also confirm insensitivity of the growth rates identified in Section 4 for $N = 8$. Coefficients of spherical harmonic expansion are represented as a column vector $\vec{\mathbf{s}} = \{a_{nm}^{(i)}, b_{nm}^{(i)}\}$, where $i = 1, 2, 3$ indexes the coordinate direction and $n \geq m$ index the spectral expansion coefficients from (1). The corresponding collocation points from (1) are $\vec{\mathbf{x}} = \{x^{(i)}(\theta_k, \phi_l)\}$, where $\theta_l \in (0, \pi)$ for $l = 1, \ldots, N$ are the colatitudinal Gauss points, and $\phi_m \in [0, 2\pi)$ for $m = 1, \ldots, 2N$ are the equally spaced and periodic longitudinal points. The forward and reverse spherical harmonic transformations between $\vec{\mathbf{x}}$ and $\vec{\mathbf{s}}$ are represented by matrices $\mathbf{B}$ and $\widetilde{\mathbf{B}}$, respectively, as defined by (1).

The Reynolds number of capsule flows is generally small, so we model the flow as governed by the Stokes equations and the capsule surface velocity $\vec{\mathbf{u}}(\vec{\mathbf{x}})$ can be represented with standard boundary integral methods [46–48]. Here, the Stokeslet Green's function is evaluated explicitly for all interactions. Boundary integrals are approximated through a quadrature scheme for the Gauss points as deduced by the spherical harmonics [44,49]. Once the velocity has been computed, the capsule membrane is advanced according to

$$\frac{\mathrm{d}\vec{\mathbf{x}}}{\mathrm{d}t} = \vec{\mathbf{u}}(\vec{\mathbf{x}}), \tag{2}$$

which for simulations we integrate using a first-order explicit method with time step $\Delta t = 10^{-4}T$.

2.3. Base capsule motion

Capsules are initiated with their centroid at the stagnation point $\mathbf{x} = 0$ and then subject to the oscillating flow (specific formula in Fig. 1) for the selected Wi and De. The period of the capsule motion is also T, since without inertia the elastic membrane responds instantaneously to the local fluid velocity.

An example single period of the capsule motion is shown in Fig. 2. The capsule is spherical at integer multiples of $T/2$, and stretches in the $\hat{\mathbf{x}}$- and $\hat{\mathbf{y}}$-directions accordingly at other times. We construct the corresponding base flow for 108 cases, with Wi ranging from 0.1 to 4 and De ranging from 0.006 to 0.2, covering the range typically probed experimentally [15]. These flows are analyzed with the non-modal Floquet analysis described in the following section.

3. Linear stability analysis

The time-periodic base configurations motivate Floquet analysis. Our formulation follows that recently developed for capsules flowing in channels [50] and tubes [51], and capsules in homogeneous shear flow [52], however for the present goals it is extended to include non-modal and time-global effects. The basic formulation is summarized in Section 3.1, and the extension is developed in Section 3.2.

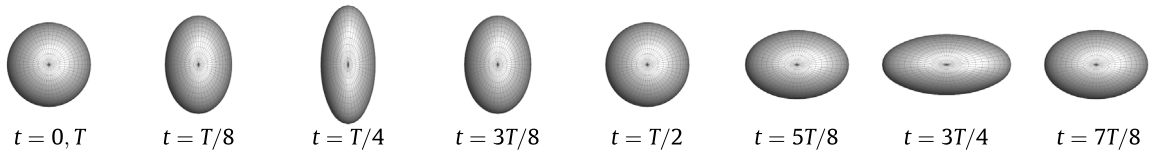

Fig. 2. Periodic base-flow conformations for $Wi = 0.8$ and $De = 0.03$.

3.1. Linearization and asymptotic analysis

Our stability analysis is cast in terms of the spherical harmonic coefficients $\vec{\mathbf{s}}$, which give a well-defined geometric measure of perturbation amplitude to the capsule membrane [51,52]. We introduce $\vec{\delta}[t]$ as a small perturbation to these coefficients and linearize about the base capsule motion. Expanding (2) and linearizing (omitting $\mathcal{O}(\|\vec{\delta}[t]\|^2)$ and higher-order terms) yields

$$\mathbf{A}[t]\,\vec{\delta}[t] = \widetilde{\mathbf{B}}\{\vec{\mathbf{u}}(\mathbf{B}\{\vec{\mathbf{s}}[t] + \vec{\delta}[t]\}) - \vec{\mathbf{u}}(\mathbf{B}\vec{\mathbf{s}}[t])\}, \tag{3}$$

where $\mathbf{A}[t]$ includes the first-order coupling between the fluid-membrane coupled base flow and the perturbation. In our computations a full-rank orthogonal set of perturbations $\vec{\delta}_i[t_j]$, each with magnitude $\delta = 10^{-3} r_o$, are used to compute each column of $\mathbf{A}[t_j]$. This process is repeated at 10^4 uniformly-spaced discrete times over the period $t_j \in [0, T)$. The evolution of a small perturbation $\vec{\boldsymbol{\varepsilon}}$ is then

$$\frac{\mathrm{d}\vec{\boldsymbol{\varepsilon}}[t]}{\mathrm{d}t} = \mathbf{A}[t]\vec{\boldsymbol{\varepsilon}}[t]. \tag{4}$$

The solution of (4) can be expressed as [53,54]

$$\vec{\boldsymbol{\varepsilon}}[t] = \mathbf{X}[t]\vec{\boldsymbol{\varepsilon}}_o, \tag{5}$$

where $\vec{\boldsymbol{\varepsilon}}_o$ is the initial condition. Periodicity requires $\mathbf{X}[t+T] = \mathbf{X}[t]\mathbf{C}$, where $\mathbf{C}$ is the monodromy matrix [53,54]. Upon substituting (5) into (4), we see that evolution of $\mathbf{X}[t]$ is

$$\frac{\mathrm{d}\mathbf{X}[t]}{\mathrm{d}t} = \mathbf{A}[t]\mathbf{X}[t]. \tag{6}$$

Here $\mathbf{X}[T]$ and, thus $\mathbf{C}$, are determined by integrating (6) with initial condition $\mathbf{X}[0] = \mathbf{I}$ using the centered trapezoidal rule, which is chosen to preserve time-reversibility.

In general, $\mathbf{C}$ is real and non-normal ($\mathbf{C}^\top\mathbf{C} \neq \mathbf{C}\mathbf{C}^\top$), so it will not have a full set of orthogonal eigenvectors. Though not diagonalizable, the eigenvalues of $\mathbf{C}$, called Floquet multipliers and denoted by ρ_i, do indicate the $t \to \infty$ behavior of small perturbations to the linearized system [55]. Thus, they provide the asymptotic growth or decay of a perturbation $\|\vec{\boldsymbol{\varepsilon}}[t]\|$ per period, with $|\rho_i| > 1$ indicating asymptotic instability. Analysis of the finite-time transient non-modal linear behavior of $\|\vec{\boldsymbol{\varepsilon}}[t]\|$ requires additional development, which is considered next.

3.2. Non-modal and global analysis of transient growth

For perturbation $\vec{\boldsymbol{\varepsilon}}_o$, the solution at any integer multiple of the period j is

$$\vec{\boldsymbol{\varepsilon}}_j \equiv \vec{\boldsymbol{\varepsilon}}[jT] = \mathbf{C}^j\,\vec{\boldsymbol{\varepsilon}}_o, \tag{7}$$

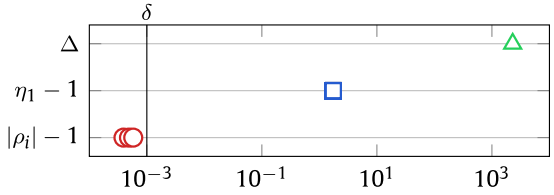

Fig. 3. Largest 3 $|\rho_i|$, η_1, and Δ discussed in text for $Wi = 0.8$ and $De = 0.03$.

and the largest possible factor of growth after j periods for non-normal components is

$$\eta_j = \max_{\vec{\boldsymbol{\varepsilon}}_o} \frac{\|\vec{\boldsymbol{\varepsilon}}_j\|}{\|\vec{\boldsymbol{\varepsilon}}_o\|} = \max_{\vec{\boldsymbol{\varepsilon}}_o} \frac{\|\mathbf{C}^j\vec{\boldsymbol{\varepsilon}}_o\|}{\|\vec{\boldsymbol{\varepsilon}}_o\|} = \|\mathbf{C}^j\| \quad , \tag{8}$$

where $\max_{\vec{\boldsymbol{\varepsilon}}_o}$ indicates the maximum over possible perturbations $\vec{\boldsymbol{\varepsilon}}_o$ and $\|\cdot\|$ is the largest singular value. As such, $\|\mathbf{C}^j\| > 1$ indicates transient amplification, though this growth is bounded by $\max|\rho_i|$ for $t \to \infty$. In traditional normal-mode stability analysis the maximum possible transient amplification is bounded by the so-named numerical abscissa [56]; we use this terminology here for the maximum observed growth after one period, which is $\eta \equiv \eta_1$ in the present notation. The associated singular vector $\vec{\mathbf{v}}_\eta$ gives the form of this growth.

The linear behavior of $\|\vec{\boldsymbol{\varepsilon}}[t]\|$ is bounded at any t, not just an integer multiple of the period, through $\mathbf{X}[t]$ [55]. Thus, the largest possible growth within the first period is

$$\Delta \equiv \max_{t_j \in [0,T]} \left\|\mathbf{X}[t_j]\right\|_1. \tag{9}$$

This metric identifies components that amplify within the period, but return to their initial amplitude at integer multiples of the period. They are thus not directly related to $\eta_{j,1}$ or ρ_i. Note that even large Δ does not necessarily indicate a linear instability from one period to the next, though if it is so large as to amplify an initially small disturbance to the r_o (capsule) scale, for which the linearization can be anticipated to fail, it will have consequences for devices that operate on them. The singular vector associated with Δ is $\vec{\mathbf{v}}_\Delta$ and experiences transient growth to amplitude $\|\vec{\boldsymbol{\varepsilon}}(t_{\max})\| = \Delta\hat{\varepsilon}$.

4. Results

We first compute ρ, η, and Δ and verify our stability analysis for the base flows described in Section 2.3. Results are shown for an example case in Fig. 3. We see $0 < |\rho_i| - 1 < \delta$, so our formulation can only establish near asymptotic neutral stability. This is because $\mathbf{C}$ and its eigenvalues are only accurate to within the δ used to construct $\mathbf{A}[t_j]$. Of course smaller δ, even more precisely determined base flows, and smaller time steps could determine these values more precisely. However, this is challenging and likely unimportant. Were such a $0 < |\rho_i| - 1 < \delta$ instability to exist, it would require at least 2000 T-periods to amplify by a factor of 10. So, in this case, there are three effectively neutral ($|\rho_i| \approx 1$) Floquet multipliers. The associated eigenvectors are rigid-body-like rotations of the capsule, for which this flow system is invariant, so their neutral stability is unsurprising. All other Floquet multipliers are small, with $|\rho_i| < 10^{-8}$ per the precision of the methods, and thus do not impact the stability conclusions [52]. More evident is the $\eta_1 = 2.74 > 1$, indicating transient amplification and taking the form of a membrane deformation. Lastly, the intra-period growth bound $\Delta \approx 2000$ is significantly larger; we will show that this value is associated with a translational capsule perturbation.

The formulation and its implementation are verified through comparison with a small-amplitude perturbation to a direct numerical simulation (DNS) in Fig. 4, which also serve to illustrate the phenomenology. The linear theory and DNS match closely for

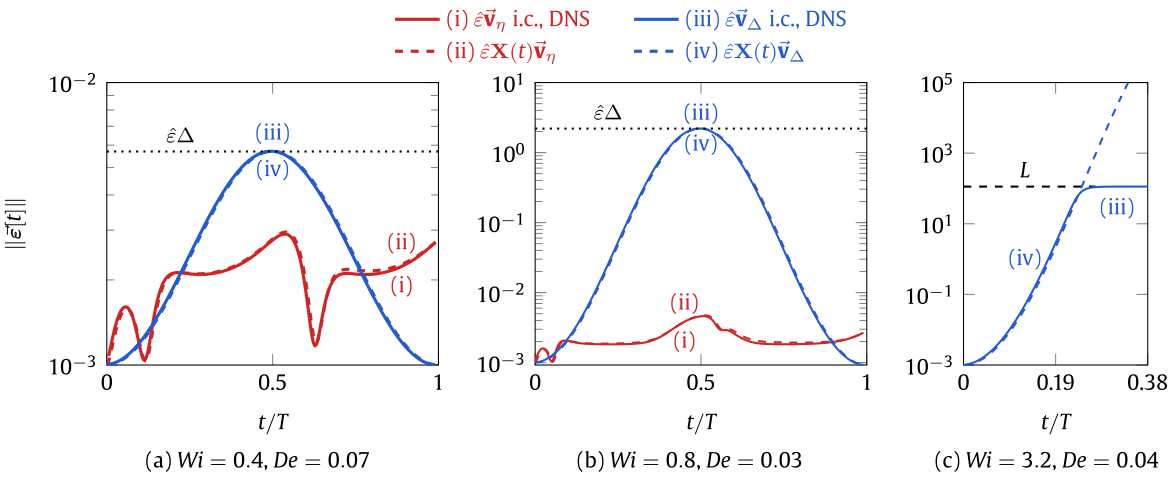

Fig. 4. Linear theory and DNS for $\vec{\mathbf{v}}_\eta$ and $\vec{\mathbf{v}}_\Delta$ over one period for cases (a)–(c) as labeled.

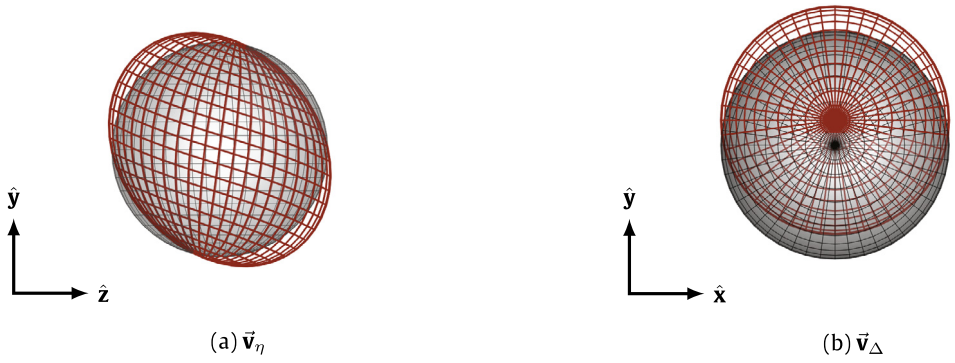

Fig. 5. Visualization of (a) $\vec{\mathbf{v}}_\eta$ and (b) $\vec{\mathbf{v}}_\Delta$ for $Wi = 0.8$ and $De = 0.03$. Perturbations are magnified as $\vec{\mathbf{s}}[0] + 5\vec{\mathbf{v}}$.

all cases and initial conditions. A large intra-period amplification $\Delta > \eta$ is observed in each case. However, this behavior is neutral period-to-period, so it will only be important if it triggers nonlinear growth, or is sufficiently large to disrupt viewing of the capsule, for instance, in an experiment. An example of a large Δ is shown in Fig. 4(c), with $\vec{\mathbf{v}}_\Delta$ amplifying about $10^5 r_o$ before the capsule (in this case) leaves the computational domain of size L. We see $\vec{\mathbf{v}}_\eta$ does have finite amplification after one period, as expected, though this growth is transient and cannot amplify quicker than that of the largest Floquet multiplier, which is effectively neutral for the cases considered. We note that there is no direct link between the asymptotic growth associated with the Floquet multipliers ρ_i and the $\vec{\mathbf{v}}_\eta$ we identify here.

Example singular vectors $\vec{\mathbf{v}}_\eta$ and $\vec{\mathbf{v}}_\Delta$ are shown in Fig. 5. The $\vec{\mathbf{v}}_\eta$ appears as a shear-like deformation in the $\hat{\mathbf{y}}$–$\hat{\mathbf{z}}$ plane; this membrane shape deformation is consistent with previous studies of transiently unstable capsule perturbations [50,51]. The $\vec{\mathbf{v}}_\Delta$ appears as a translation of the capsule in the $\hat{\mathbf{y}}$-direction. Indeed this growth can be anticipated, as the flow is in extension in one of the coordinate directions at any given time, which is fundamentally unstable. The direction of this amplification switches every half-period, resulting in the neutral behavior observed in Fig. 4. We analyze this intra-period amplification next.

Example Δ are shown in Fig. 6(a). We see Δ increases with Wi and $1/De$, which can be anticipated as the strength and duration of the flow and its period increase, respectively. The increase of Δ with $1/De$ is exponential with rate α for constant Wi. Further, α

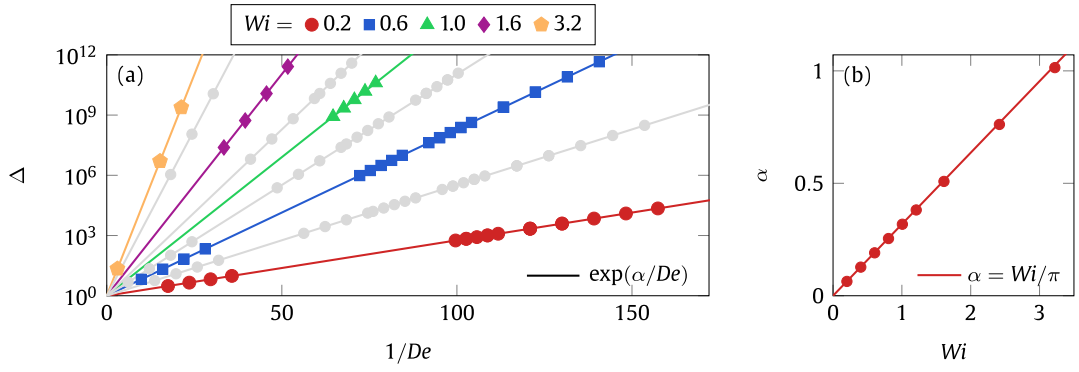

Fig. 6. (a) Δ for varying De and Wi. (b) Linear least-squares fitted α for $\Delta = \exp(\alpha/De)$ at select Wi.

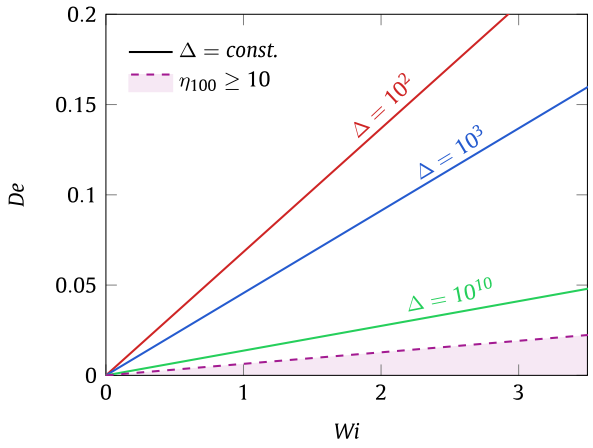

Fig. 7. Pipkin space showing contours of constant Δ and η_{100} as labeled.

increases linearly with Wi (with slope $1/\pi$), as shown in Fig. 6(b). These observations can be expressed compactly as

$$\Delta = \exp\left(\frac{Wi}{\pi De}\right). \tag{10}$$

This result is consistent with the displacement of a rigid, infinitesimal, particle perturbed in an analogous one-dimensional oscillatory extensional flow, as deduced from the governing equation of such a particle,

$$\frac{\mathrm{d}x}{\mathrm{d}t} = \dot{\epsilon}_0 \sin(2\pi t/T)x, \tag{11}$$

where x is the particle position. This has solution

$$x(t) = \exp\left(\frac{\dot{\epsilon}_0 T}{2\pi}\left[1 - \cos\left(2\pi t/T\right)\right]\right)\delta, \tag{12}$$

where δ is the initial perturbation amplitude. It is evident that the largest amplification occurs when $t = T/2$ or $3T/2$, so $\Delta = \exp(\dot{\epsilon}_0 T/\pi)$, which is consistent with (10) and the $1/\pi$ slope seen in Fig. 6(b). Thus, the elasticity of the capsule membrane is ultimately unimportant for the translational intra-period amplification we identify, and the capsule behaves very nearly as an infinitesimal particle when subject to this translation in LAOE flow.

We use (10) to cast isocontours of Δ onto a *Wi*–*De* Pipkin space [57], as shown in Fig. 7, to compare the relative amplifications we observe. The locus of cases that satisfy $\eta_{100} > 10$; that is, cases that could amplify a perturbation by a factor of ten within 100 T-periods through a transient mechanism, are shown to facilitate this comparison. We see $\eta_{100} > 10$ for only large Wi and small De, which is much smaller than Δ for the same cases. We thus conclude that the transient amplification we observe is subservient to the translational intra-period growth.

Lastly, we consider capsule membrane with spatially non-uniform elasticity; this serves as a model for actual capsules that do not have exactly uniform elasticity. We vary the shear modulus linearly in the $\hat{\mathbf{y}}$ direction:

$$\widetilde{E}_s(\mathbf{x}) = E_s\left(1 + \frac{gy}{r_o}\right), \tag{13}$$

where g is the strength of the non-uniformity. The single-period amplification of a capsule with shear elasticity $\widetilde{E}_s$ from $\varepsilon = 0$ is shown in Fig. 8. The maximum growth increases linearly with g for constant Wi for all cases considered, consistent with the linear variation in $\widetilde{E}_s$ with g. $\|\vec{\boldsymbol{\varepsilon}}_1\|$ increases monotonically, though not linearly, with Wi for constant g. In all cases, even for large g, the amplification is relatively small, with $\|\vec{\boldsymbol{\varepsilon}}_1\| < 0.1r_o$, compared with the larger Δ associated with translational perturbations $\vec{\mathbf{v}}_\Delta$.

5. Discussion and conclusions

A non-modal and time-global Floquet stability analysis was formulated for fully-coupled capsule-viscous-flow systems, extending previous studies of time-stationary capsule flows. This analysis was applied to the motion of (at-rest) spherical capsules subject to LAOE flow of varying strength and frequency. All flow strengths and periods were found to be $t \to \infty$ stable, a result shared with initially spherical vesicles in time-stationary extensional flow [30]. A set of transiently amplifying perturbations, however, were identified in each case. These perturbations include shape distortions of the capsule membrane, similar to other transiently unstable capsule flows [50,51]. Here, transiently unstable perturbations amplified slowly over many periods, as demonstrated by the only small fraction of cases that satisfied $\eta_{100} > 10$. Further, this growth necessarily saturates at long times due to their asymptotic stability. Thus, this transient amplification is likely unimportant in application.

An intra-period transient amplification Δ was also identified. It was associated with a translation of the capsule and amplified many orders of magnitude in certain cases, depending on the flow strength and period. This amplification was associated a shift of the flow stagnation point, and was thus consistent with that of a rigid particle in the same flow. As a result, the elasticity of the capsule membrane was subservient to the hydrodynamic behavior. Importantly, this capsule translation did not amplify on a period-to-period basis, as precluded by its asymptotic stability. Ultimately, this perturbation is only important if it is not damped through a flow control mechanism. Further, since it did not involve membrane deformations, only translational flow control is required. Such a control mechanism has been successfully

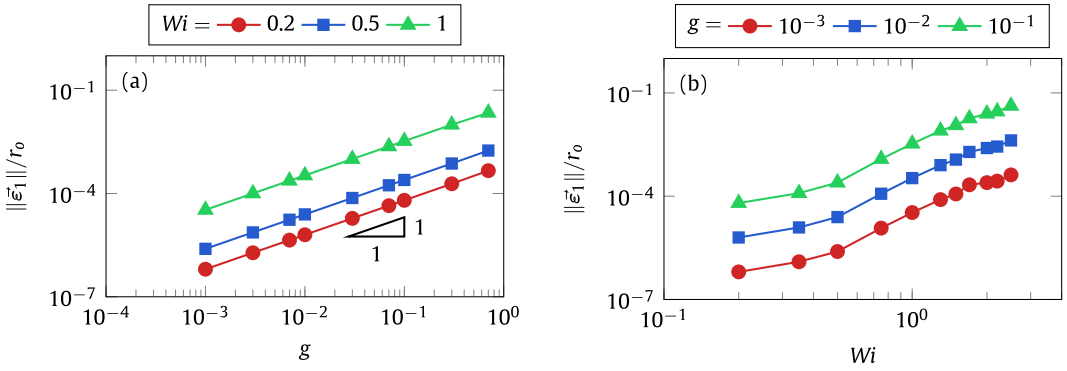

Fig. 8. Disturbance amplitude $\|\vec{\boldsymbol{\varepsilon}}_1\|$ for capsules with non-uniform shear elasticity for varying (a) g and (b) Wi. All cases have $De = 0.1$.

implemented for single strands of DNA by shifting the stagnation point of the flow [14,15]. This is in contrast to a more complex flow field control that would be required to damp more complex perturbations, such as those involving high-order deformations of the membrane.

Lastly, we showed that these translational perturbations have larger amplification than do perturbations arising from spatially non-uniform membrane elasticity. We thus conclude that such translational disturbances are of principal importance when considering the stability of such a particle in LAOE flow, even when considering the possible non-uniformity (and, thus, asymmetry) of actual capsules.

Acknowledgment

This work was supported in part by the National Science Foundation, USA under Grant No. CBET 13-36972.

References

[1] J.G. Nam, K. Hyun, K.H. Ahn, S.J. Lee, Prediction of normal stresses under large amplitude oscillatory shear flow, J. Non-Newton. Fluid Mech. 150 (1–10) (2008).
[2] D. Chopra, D. Vlassopoulos, S.G. Hatzikiriakos, Nonlinear rheological response of phase separating polymer blends: poly-(styrene-co-maleic anhydride)/poly(methyl methacrylate), J. Rheol. 44 (2000) 27–45.
[3] B. Debbaut, H. Burhin, Large amplitude oscillatory shear and fourier-transform rheology for a high-density polyethylene, J. Rheol. 46 (1155) (2002).
[4] C.O. Klein, H.W. Spiess, A. Calin, C. Balan, M. Wilhelm, Separation of the nonlinear oscillatory response into a superposition of linear, strain hardening, strain softening, and wall slip response, Macromolecules 40 (2007) 4250–4259.
[5] P.C. Sousa, J. Carneiro, R. Vaz, A. Cerejo, F.T. Pinho, M.A. Alves, M.S.N. Oliveira, Shear viscosity and nonlinear behavior of whole blood under large amplitude oscillatory shear, Biorheology 50 (5–6) (2013) 269–282.
[6] G. Tomaiuolo, A. Carciati, S. Caserta, S. Guido, Blood linear viscoelasticity by small amplitude oscillatory flow, Rheol. Acta 55 (6) (2016) 485–495.
[7] G.H. Mckinley, T. Sridhar, Filament-stretching rheometry of complex fluids, Ann. Rev. Fluid Mech. 34 (2002) 375–415.
[8] H.K. Rasmussen, P. Laillè, K. Yu, Large amplitude oscillatory elongation flow, Rheol. Acta 47 (2008) 97–103.
[9] A.G. Bejenariu, H.K. Rasmussen, A.L. Skov, O. Hassager, S.M. Frankaer, Large amplitude oscillatory extension of soft polymeric networks, Rheol. Acta 49 (2010) 807–814.
[10] S.J. Haward, M.S.N. Oliveira, M.A. Alves, G.H. McKinley, Optimized cross-slot flow geometry for microfluidic extensional rheometry, Phys. Rev. Lett. 109 (2012) 1–5.
[11] S.J. Haward, V. Sharma, J.A. Odell, Extensional opto-rheometry with biofluids and ultra-dilute polymer solutions, Soft Matter 7 (9908) (2011).
[12] S.J. Haward, J.A. Odell, Z. Li, X.F. Yuan, Extensional rheology of dilute polymer solutions in oscillatory cross-slot flow: The transient behavior of birefringent strands, Rheol. Acta 49 (2010) 633–645.
[13] J.A. Odell, S.P. Carrington, Extensional flow oscillatory rheometry, J. Non-Newton. Fluid Mech. 137 (2006) 110–120.
[14] Y. Zhou, C.M. Schroeder, Transient and average unsteady dynamics of single polymers in large-amplitude oscillatory extension, Macromolecules 49 (8018–8030) (2016).
[15] Y. Zhou, C.M. Schroeder, Single polymer dynamics under large amplitude oscillatory extension, Phys. Rev. Fluids 1 (053301) (2016).
[16] I.M. Martins, M.F. Barreiro, M. Coelho, A.E. Rodrigues, Microencapsulation of essential oils with biodegradable polymeric carriers for cosmetic applications, Chem. Eng. J. 245 (2014) 191–200.
[17] K. Miyazawa, I. Yajima, I. Kaneda, T. Yanaki, Preparation of a new soft capsule for cosmetics, J. Cosmet. Sci. 51 (4) (2000) 239–252.
[18] B.F. Gibbs, S. Kermasha, I. Alli, C.N. Mulligan, Encapsulation in the food industry: a review, Int. J. Food Sci. and Neut. 50 (1999) 213–224.
[19] F. Pop, Chemical stabilization of oils rich in long-chain polyunsaturated fatty acids during storage, Food Sci. Technol. Int. 17 (2) (2011) 111–117.
[20] G. Ma, Z. Su, Microspheres and Microcapsules in Biotechnology: Design, Preparation and Applications, Pan Stanford, 2013.
[21] J.J. Vericella, S.E. Baker, J.K. Stolaroff, E.B. Duoss, J.O.H. IV, J. Lewicki, E. Glogowski, W.C. Floyd, C.A. Valdez, W.L. Smith, J.H. Satcher Jr, W.L. Bourcier, C.M. Spadaccini, J.A. Lewis, R.D. Aines, Encapsulated liquid sorbents for carbon dioxide capture, Nature Commun. 6 (6124) (2015).
[22] N.S. Dey, S. Majumdar, M.E.B. Rao, Multiparticulate drug delivery systems for controlled release, Trop. J. Pharm. Res. 7 (3) (2008) 1067–1075.
[23] N. Paret, A. Trachsel, D.L. Berthier, A. Herrmann, Controlled release of encapsulated bioactive volatiles by rupture of the Capsule wall through the light-induced generation of a gas, Chem. Int. Ed. 54 (7) (2015) 2275–2279.
[24] F. Lim, Biomedical Applications of Microencapsulations, Boca Raton, FL: CRC, 1984.
[25] N.J. Zuidam, V. Nedovic, Encapsulation Technologies for Active Food Ingredients and Processing, New York: Springer, 2010.
[26] B. Furlow, Contrast-enhanced ultrasound, Radiol. Technol. 80 (2009) 547–561.
[27] W.M. Kuhtreiber, R.P. Lanza, W.L. Chick, Cell Encapsulation Technology and Therapeutics, Birkhauser, 1998.
[28] T.M. Chang, Blood replacement with nanobiotechnologically engineered hemoglobin and hemoglobin nanocapsules, Wiley Intersci. Rev. Nanomed. Nanobiotechnol. 2 (2010) 418–430.
[29] H.A. Clayton, R.F.L. James, N.J.M. London, Islet microencapsulation: a review, Acta Diabetol. 30 (1993) 181–189.
[30] H. Zhao, E.S.G. Shaqfeh, The shape stability of a lipid vesicle in a uniaxial extensional flow, J. Fluid Mech. 719 (2013) 345–361.
[31] V. Narsimhan, A.P. Spann, E.S.G. Shaqfeh, The mechanism of shape instability for a vesicle in extensional flow, J. Fluid Mech. 750 (2014) 144–190.
[32] V. Narsimhan, A.P. Spann, E.S.G. Shaqfeh, Pearling, wrinkling, and buckling of vesicles in elongational flows, J. Fluid Mech. 777 (2015) 1–26.
[33] P. Dimitrakopoulos, Dumbbell formation for elastic capsules in nonlinear extensional Stokes flows, Phys. Rev. Fluids 2 (6) (2017) 063101.
[34] J.B. Dahl, V. Narsimhan, B. Gouveia, S. Kumar, E.S.G. Shaqfeh, S.J. Muller, Experimental observation of the asymmetric instability of intermediate-reduced-volume vesicles in extensional flow, Soft Matter 12 (3787) (2016).
[35] L. Guillou, J.B. Dahl, J.G. Lin, A.I. Barakat, J. Husson, S.J. Muller, S. Kumar, Measuring cell viscoelastic properties using a microfluidic extensional flow device, Biophys. J. 111 (2016) 2039–2050.
[36] J. Dupire, M. Abkarian, A. Viallat, Chaotic dynamics of red blood cells in a sinusoidal flow, Phys. Rev. Lett. 104 (168101) (2010).
[37] L. Zhu, J. Rabault, L. Brandt, The dynamics of a capsule in a wall-bounded oscillating shear flow, Phys. Fluids 27 (2015) 071902.
[38] D. Cordasco, P. Bagchi, Dynamics of red blood cells in oscillating shear flow, J. Fluid Mech. 800 (2016) 484–516.
[39] J. Dupire, M. Socol, A. Viallat, Full dynamics of a red blood cell in shear flow, Proc. Natl. Acad. Sci. USA 109 (51) (2012) 20808–20813.
[40] C. Dupont, F. Delahaye, D. Barthes-Biesel, A.-V. Salsac, Stable equilibrium configurations of an oblate capsule in simple shear flow, J. Fluid Mech. 791 (2016) 738–757.
[41] C. Dupont, A.-V. Salsac, D. Barthès-Biesel, Off-plane motion of a prolate capsule in shear flow, J. Fluid Mech. 721 (2013) 180–198.
[42] J. Walter, A.-V. Salsac, D. Barthès-Biesel, Ellipsoidal capsules in simple shear flow: prolate versus oblate initial shapes, J. Fluid Mech. 676 (2011) 318–347.
[43] R. Skalak, A. Tozeren, P.R. Zarda, S. Chien, Strain energy function of red blood cell membranes, Biophys. J. 13 (1973) 245.
[44] H. Zhao, A.H.G. Isfahani, L. Olson, J.B. Freund, A spectral boundary integral method for micro-circulatory cellular flows, J. Comput. Phys. 229 (2010) 3726–3744.
[45] A. Guckenberger, S. Gekle, Theory and algorithms to compute helfrich bending forces: a review, J. Phys. Condens. Matter 29 (20) (2017) 203001.
[46] S. Kim, S.J. Karrila, Microhydrodynamics: Principles and Selected Applications, Butterworth-Heinemann, Boston, 1991.
[47] C. Pozrikidis, Boundary Integral and Singularity Methods for Linearized Viscous Flow, Cambridge University Press, Cambridge, 1992.
[48] J.M. Rallison, A. Acrivos, A numerical study of the deformation and burst of a viscous drop in an extensional flow, J. Fluid Mech. 89 (1978) 191–200.
[49] J.B. Freund, H. Zhao, A fast high-resolution boundary integral method for multiple interacting blood cells, in: C. Pozrikidis (Ed.), Hydrodynamics of Capsules and Biological Cells, Chapman and Hall/CRC, Boca Raton, FL, 2010, pp. 71–111.
[50] S.H. Bryngelson, J.B. Freund, Capsule-train stability, Phys. Rev. Fluids 1 (3) (2016) 033201.
[51] S.H. Bryngelson, J.B. Freund, Global stability of flowing red blood cell trains, Phys. Rev. Fluids 3 (7) (2018) 073101.
[52] S.H. Bryngelson, J.B. Freund, Floquet stability analysis of capsules in viscous shear flow, J. Fluid Mech. 852 (2018) 663–677.
[53] F. Verhulst, Nonlinear Differential Equations and Dynamical Systems, Berlin: Springer–Verlag, 2006.
[54] J. Liu, A First Course in the Qualitative Theory of Differential Equations, Englewood Cliffs, NJ: Prentice Hall, 2003.
[55] P.J. Schmid, Nonmodal stability theory, Annu. Rev. Fluid Mech. 39 (2007) 129–162.
[56] L.N. Trefethen, Pseudospectra of linear operators, SIAM Rev. 39 (3) (1997) 383–406.
[57] A.C. Pipkin, Lectures on Viscoelastic Theory, Springer-Verlag New York, 1972.